XVIII IMEKO WORLD CONGRESS
Metrology for a Sustainable Development
September, 17 – 22, 2006, Rio de Janeiro, Brazil

HOLLOW BEAM GEOMETRY FOR DIFFUSING TEMPORAL LIGHT CORRELATION

Luigi Rovati , Nicola Zambelli, Stefano Cattini and Giorgia Salvatori

Department of Information Engineering, University of Modena and Reggio Emilia, Modena, Italy, rovati.luigi@unimo.it

Abstract: The paper presents an optical setup for diffusing temporal light spectroscopy of living tissues. The system allows to study the dynamical properties of living tissues molecules. The proposed approach exploits the hollow beam geometry in conjunction to mode-selective detection. First experiments, aimed to demonstrate the functionality of the measuring system, have been performed.

Keywords: Diffusing temporal light spectroscopy, hollow beam geometry, biomedical optics.

1. INTRODUCTION

The knowledge of the dynamical properties of molecules in living tissues yields important information. Temporal variations in the amplitude and phase of diffused photons can be used to derive such information. Scattering is originated by a mixture of macromolecules, which are rigidly fixed into the structural matrix of the tissue or can move. The motion of these molecules depends on various parameters, such as shape and size of the molecules, interaction among other molecules, constraints due to membranes, and so forth.

In the past decades, to characterize dynamical properties of weakly scattering media, dynamic light scattering (DLS) has been used extensively [1]. However living tissue are highly scattering materials and, during the multiple scattering events, details about sample properties are lost. The intensity of the multiple scattered light can be accurately predicted by the photon diffusion equation according to the diffusing wave spectroscopy theory. The associated technique is known as diffusing temporal light correlation (DTLC) and represents the extension of the DLS to the highly diffusing media [2].

The basic optical setup is similar for the two techniques, however the signal amplitude recovered in the DTLC method decreases exponentially with the distance d between the illumination and collection point. The distribution of photons, which travel through the tissue from the illumination point to the collection site, is a banana shaped volume called banana function that has a maximum depth into the tissue proportional to $\sqrt{d}$. Thus, DTLC approach is practically usable only to study superficial properties of the tissue since, increasing distance d, the signal is rapidly lost into the background noise. In our previous paper [3], we proposed a hollow beam geometry to improve the sensitivity of DLS; here the same optical setup is used to extend the tissue depth investigable using DTLC.

2. METHODS

Non-invasive determination of the molecules motion properties in living tissues by DTLC requires the study of the intensity fluctuations of the scattered light. In the next sections, we first introduce a theoretical description of the problem and afterward the experimental setup used in this study.

2.1 Basic theory

Consider the simplified optical layout reported in Figure 1. Living tissue is illuminated by a hollow laser beam. Photons migrate through the tissue and some of them are collected at the centre of the ring of radius ρ projected onto the tissue. Absorption and scattering are the major phenomena governing photons propagation through the tissue. Absorption effects are described by the absorption coefficient $\mu_a(\lambda)$ whereas scattering effects are described by the reduced scattering or transport scattering coefficient $\mu'_s(\lambda)=(1-g)\mu_s(\lambda)$; where $\mu_s(\lambda)$ is the reciprocal of the mean distance between scattering events, and g is the mean cosine of the scattering angle or scattering phase function.

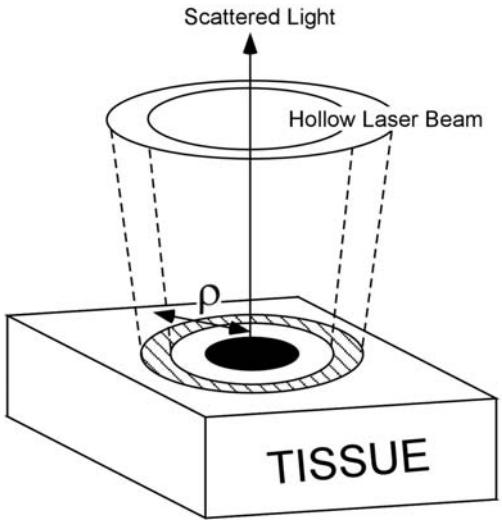

Fig. 1. Simplified optical layout of the hollow beam geometry.

The motions of scatterers can be characterized by the normalized electric field autocorrelation function:

$$g_1(\tau) = \frac{\langle E(0) \cdot E(\tau) \rangle}{\langle E(0)^2 \rangle}, \quad (1)$$

where E is the electric field of the scattered light.

Experimentally, this information can not be acquired directly but can be derived by the intensity autocorrelation function. In the case of mode-selective detection (as realized with a single-mode collection fiber), the intensity autocorrelation function can be written as [4]

$$g_2(\tau) = \frac{\langle I(0) \cdot I(\tau) \rangle}{\langle I(0)^2 \rangle}, \quad (2)$$

$$g_2(\tau) = 1 + \frac{h}{(1+h)^2} \mathrm{Re}[g_1(\tau)] + \frac{1}{(1+h)^2} |g_1(\tau)|^2$$

where I is the intensity of the scattered light, and *h* is the heterodyne parameter defined as

$$h = \frac{I_{sl}}{\langle I_d \rangle} \cdot \quad (3)$$

I_{sl} is the intensity of the static stray light that is originated by the scattering of static scattering centres, whereas $\langle I_d \rangle$ is the temporal average intensity scattered by moving molecules [4]. The parameter *h* can be evaluated from the intensity autocorrelation function according to the relation

$$h = \frac{1}{g_2(0) - 1} - 1 \cdot \quad (4)$$

The electric field autocorrelation function in heterogeneous tissues can be calculated solving the diffusion equation [2]:

$$\left[\nabla^2 - 3 \cdot \mu_a \cdot \mu_s' + \right.$$
$$\left. - \mu_s'^2 \cdot k_o^2 \cdot \alpha \cdot \langle \Delta r^2(\tau) \rangle \right] \cdot g_1(\tau) = -3\mu_s' \frac{S(r)}{\langle I_d \rangle}, \quad (5)$$

where k_0 is the wavenumber of the photons in the medium, $\langle \Delta r^2(\tau) \rangle$ is the mean square displacement of the scatterers during the time interval τ, α represents the probability that the light scattering event is with a moving scetterer and S(r) is the illumination distribution.

In living tissues the motion of the scatteres can be due to (i) Brownian motion, (ii) random flow (blood flow in the capillary network) and (iii) shear flow (blood flow in the artery and vein vessels). Thus the mean square displacement of the scatterers can be expressed as

$$\langle \Delta r^2(\tau) \rangle = \left(\langle v^2 \rangle + \frac{\Gamma_{eff}^2}{5 \cdot \mu_s'^2} \right) \tau^2 + 6 D_B \tau, \quad (6)$$

where $\langle v^2 \rangle$ is the second moment of the particles speed distribution (assuming the velocity distribution to be isotropic and Guassian in the capillary network), Γ_{eff}^2 is the effective shear rate in the vessels and D_B is the Brownian diffusion coefficient of the molecules with dynamics governed by thermal effects.

Considering a semi-infinite medium, analytic solution of Eq. (5) is formally the same as for the diffuse photon density waves [5]:

$$g_1(\tau) = \left\{ r_2 \exp\left(- r_1 \sqrt{k_0^2 \mu'^2_s \cdot \alpha \langle \Delta r^2(\tau) \rangle + 3\mu_a \mu'_s} \right) + \right.$$
$$\left. - r_1 \exp\left(- r_2 \sqrt{k_0^2 \mu'^2_s \cdot \alpha \langle \Delta r^2(\tau) \rangle + 3\mu_a \mu'_s} \right) \right\} \cdot \quad (7)$$
$$\left\{ r_2 \exp\left(- r_1 \sqrt{3\mu_a \mu'_s} \right) - r_1 \exp\left(- r_2 \sqrt{3\mu_a \mu'_s} \right) \right\}^{-1}$$

where

$$r_1 = \sqrt{\rho^2 + 1/\mu_s'^2}, \quad (8)$$

and

$$r_2 \cong \sqrt{\rho^2 + 20.43/\mu_s'^2} \quad . \quad (9)$$

2.2 Instrumentation

Hollow beam DTLC measurements have been performed using the experimental setup shown in Figure 2. The Gaussian beam generated by the HeNe laser is collimated by the lens L1 and shaped using the diaphragm D. The central part of the beam is blocked by this diaphragm in order to generate a collimated donut shaped beam. Beam transmitted is then processed by the objective OBJ. The elliptic mirror M1 is drilled in the center in order to redefine the hollow excitation beam and to deflect only the peripheral part of the beam. The hole in M2 allows the confocal collection of the scattered light. The so obtained excitation beam is then focused on the target by the lens L2 and the mirror M2. The ring projected on the target has a diameter ρ=3mm.

The light scattered by the target retraces the excitation beam path through mirror M2 and lens L2. The hole in mirror M1 allows the scattered light to be collected by lens L3 and focused in the single-mode fibre F.

Fiber F is connected to a single photon counting module (SPCM) that transforms the scattered light intensity into an TTL electrical signal. The digital correlator DC (BI-9000AT, Brookhaven Instruments corp., NY, USA) plugged into a computer acquires this electrical signal and calculates the intensity autocorrelation function.

Figure 3 shows a picture of the hollow beam reflected by the mirror M2.

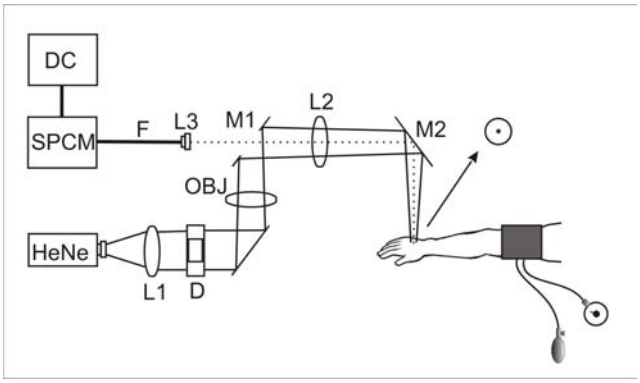

Fig. 2. Block diagram of the measuring system. HeNe: Helium-Neon Laser, L1: collimating lens, D: shaping diaphragm, OBJ: focusing objective, M1: drilled elliptical mirror, L2: focusing lens, M2: mirror, L3: collecting lens, F: single-mode fiber, SPCM: single-photon counting module, DC: digital correlator.

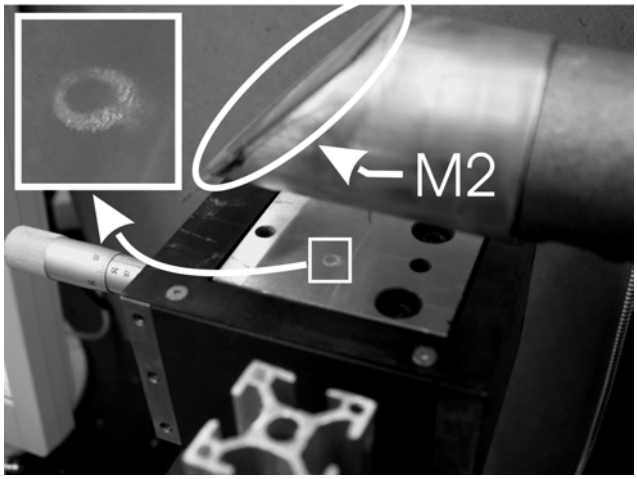

Fig. 3. Hollow beam reflected by the mirror M2.

3. RESULTS AND DISCUSSION

3.1 System characterization

To test the performance of the developed system, we used different aqueous suspensions of Intralipid (Intralipid® 20% by Fresenius Kabi) in various concentrations as tissue phantom. Intralipid is an intravenous nutrient consisting of an emulsion of phospholipids micelles and water. Because intralipid is turbid and has no strong absorption bands in the visible and Near Infrared (NIR) region of the electromagnetic spectrum, it is often exploited as a tissue simulating phantom medium in spectroscopy experiments.
In the red-NIR spectrum, Intralipid's optical properties have been studied and reported in literature by several authors [6]. The concentrations of the analyzed solutions, expressed in terms of volume fraction **Φ**, are shown in Table 1. Optical properties of the samples have been calculated from data reported in literature taking into account the actual intralipid volume fraction of our samples.
The resulting samples consist of two components: a liquid solvent and scattering phospholipids micelles. Intralipid micelles are much larger and much heavier than the water molecules, yet small enough to be subject to appreciable thermal fluctuation.
Colloidal particles moving under the action of random thermal forces in viscous fluids exhibit Brownian motion, at a sufficient long time.

Table 1. Volume fraction Φ and calculated optical property of the investigated samples. The symbols reported in the last column refer to curves shown in figure 4.

Meas.	$\Phi[V_I/V_{TOT}]$	$\mu_a[mm^{-1}]$	$\mu_s[mm^{-1}]$	Symb.
1	$4.23\cdot10^{-3}$	$3.19\cdot10^{-3}$	0.63	+
2	$8.29\cdot10^{-3}$	$3.37\cdot10^{-3}$	1.17	○
3	$12.2\cdot10^{-3}$	$3.55\cdot10^{-3}$	1.69	none
4	$15.9\cdot10^{-3}$	$3.72\cdot10^{-3}$	2.19	none
5	$19.6\cdot10^{-3}$	$3.88\cdot10^{-3}$	2.67	none
6	$23.0\cdot10^{-3}$	$4.04\cdot10^{-3}$	3.14	□
7	$26.4\cdot10^{-3}$	$4.19\cdot10^{-3}$	3.59	none
8	$29.6\cdot10^{-3}$	$4.33\cdot10^{-3}$	4.02	none
9	$32.7\cdot10^{-3}$	$4.48\cdot10^{-3}$	4.44	none
10	$35.8\cdot10^{-3}$	$4.61\cdot10^{-3}$	4.84	△

As suggested by several authors [7,8], by considering the simplified model of steric interaction among particles, the equivalent Brownian diffusion coefficient of the suspended particles is concentration dependent. Increasing the particles concentration, the direct hard-sphere interactions among the particles reduce the Brownian mean square displacement observable in the case of non-interacting particles.
As an example, figure 4 shows the electric field autocorrelation functions obtained by performing DTLC measurements on four of the analyzed samples.
As shown in figure 4, the decay time of the autocorrelation functions decreases and thus, apparently, the mean square displacement increases consequently to the increased volume fraction of Intralipid. This non-realistic interpretation is due to the effect of $\mu_s(\lambda)$ on the autocorrelation function, described by Eq. (7). As shown in Table 1, the scattering coefficient $\mu_s(\lambda)$ increases almost linearly with the volume fraction of Intralipid. Therefore, increasing the volume fraction also the average number of scattering events suffered by the revealed photons increas thus reducing the degree of correlation of the acquired signals.

To obtain the actual information concerning the mean square displacement, each of the ten experimental electric filed autocorrelation functions curves obtained by the analyzed samples was fitted by the theoretical function reported in Eq. (7) supposing the mean square displacement $\left\langle \Delta r^2(\tau) \right\rangle$ equal to $6D_B\tau$. In the fitting procedure, we set the absorption and scattering coefficients to the values reported in Table 1 and α=1. Figure 5 shows the extrapolated equivalent Brownian D_B diffusion coefficient as a function of the intralipid volume fraction. As expected, D_B decreases and thus the particles mean square displacement decreases at high concentrations of Intralipid.

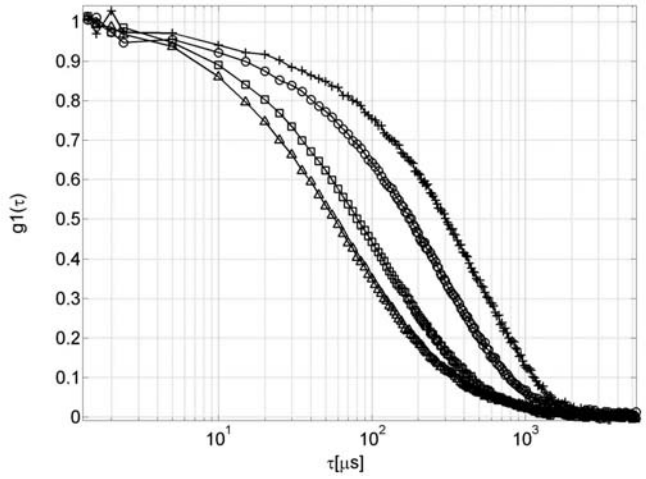

Fig. 4. Electric field autocorrelation functions obtained by performing DTLC measurements on four of the analyzed samples. The corresponding volume fraction of intralipid is reported in Table 1. The high is the intralipid concentration the short is the exponential decay time.

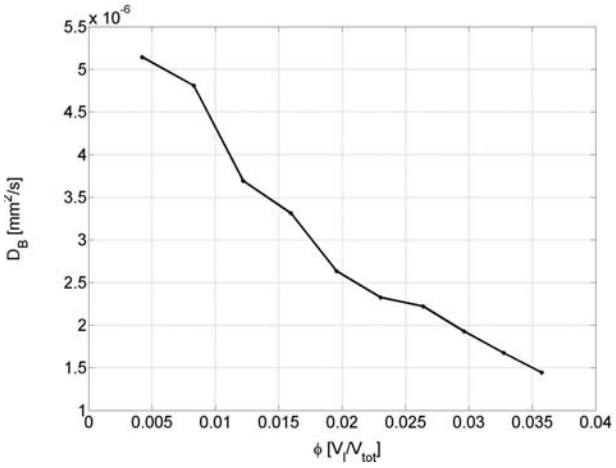

Fig. 5. Diffusion coefficient D_B as a function of the Intralipid volume fraction. The curve is obtained by fitting the experimental data with Eq. (7).

3.2 In-vivo experiment

Preliminary measurements have been acquired on a male subject aged 27 years. A sphygmomanometer cuff was placed on the left arm and the compression pressure was increased from 0 to 100 Torr as quick as possible. This pressure is sufficient to induce a partial venous occlusion and therefore a change of the blood flow in the arm vascular system. The measuring region was fix on the top of the hand far away from visible vessels, in order to study just the capillaries flow. We acquired an intensity correlation function just before inflating the cuff. The second acquisition was performed just after inflating the cuff followed by the last measurement after 3 minutes. Thanks to the hollow beam geometry we obtained a superb count rate at the output of the SPCM (average 40Kcps) in all the acquisitions. Higher count rate can be obtained changing the laser wavelength in the near-infrared region, where the tissue absorption decreases.

Figura 6 shows the electric field autocorrelation functions obtained during the experiment. Unlike the in-vitro test, the scattering properties of the sample could be considered roughly constant during the experiment. In fact, our measuring region is far away from visible vessels and thus the increase of the blood volume in the inspected tissue can be neglected.

Assuming applicable this simplification, the decay time of the autocorrelation function is related only to the changes in the mean square displacement of the scatteres.

As shown in figure 6, the decay time, of the autocorrelation functions increases in the time confirming that the mean square displacement of the scatteres decreases since the blood flow is partially blocked. Moreover note as the shape of the electric field autocorrelation function changes in the time. Before inflating the cuff, $\log(g_1(\tau))$ decreases practically linearly with τ, thus confirming the molecules motion is mainly described by the random flow model, i.e. $\langle \Delta r^2(\tau) \rangle \cong \langle v^2 \rangle \tau^2$. On the other hand, after inflating, the shape of $\log(g_1(\tau))$ can be approximated to $\sqrt{\tau}$ according to the Brownian motion model, i.e. $\langle \Delta r^2(\tau) \rangle \cong 6 D_B \tau$.

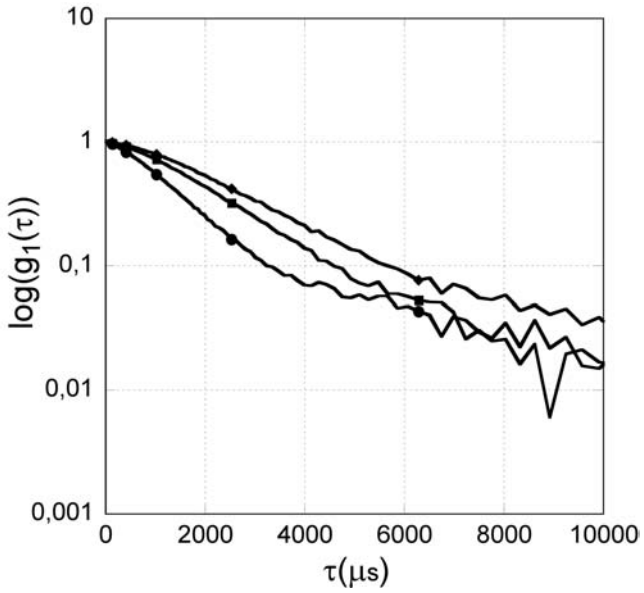

Fig. 6. Electric field autocorrelation functions obtained during the occlusion experiment. (●) Before the venous occlusion, (■) just after inflating the cuff at 100mmHg and (♦) after 3 minutes.

4. CONCLUSIONS

We proved as the hollow beam geometry can be efficiently used in diffusing temporal light correlation technique. Preliminary results on a volunteer are encouraging and confirm the theoretical expectations.

REFERENCES

[1] R. Pecora, “Dynamic Light Scattering: Applications of Photon Correlation Spectroscopy,” Plenum Press, 1985.

[2] D.A. Boas, L.E. Campell and A.G. Yodh, “Scattering and Imaging with diffusion temporal field correlations,” Phys. Rev. Lett. Vol. 75, No. 9, pp. 1855-1858, 1995.

[3] L. Rovati, "Hollow beam geometry for dynamic light scattering measurements: a theoretical analysis", App. Opt., Vol. 36, pp. 9083-9089, 1997.

[4] L. Rovati, F. Frankhauser II and J. Ricka, "Design and performance of a new ophthalmic instrument for dynamic light-scattering measurements in the human eye", Rev. Sci. Instrum., Vol. 67, pp. 2615-2620, 1996.

[5] D.A. Boas "Diffuse photon probes of structural and dynamical properties of turbid media theory and biomedical applications", Doctor of Philosophy thesis, University of Pennsylvania, 1996.

[6] S.T. Flock, S.L. Jacques, B.C. Wilson, W.M. Star and M.J.C. van Gemert, "Optical Properties of Intralipid: A phantom medium for light propagation studies," Lasers in Surgery and Medicine Vol.12, pp. 510-519, 1992.

[7] C.W.J. Beenakker and P. Mazur, "Diffusion of spheres in suspension: three-body hydrodynamic interaction effects", Phys. Rev. Lett., Vol.91, pp. 290-291, 1982.

[8] Scott T. Milner and Andrea J. Liu, "Concentration dependence of long-time tails in colloidal suspensions", Phys. Rev. E., Vol.48, pp.449-454, 1993.